Conjugation with Cationic Cell-Penetrating Peptide Increases Pulmonary Absorption of Insulin

ARTICLE *in* MOLECULAR PHARMACEUTICS · MARCH 2009

Impact Factor: 4.38 · DOI: 10.1021/mp800174g · Source: PubMed

6 AUTHORS, INCLUDING:

Kwang-Jin Kim
Keck School of Medicine USC
161 PUBLICATIONS **4,469** CITATIONS
SEE PROFILE

Edward Crandall
University of Southern California
196 PUBLICATIONS **5,135** CITATIONS
SEE PROFILE

wei-chiang Shen
University of Southern California
141 PUBLICATIONS **3,587** CITATIONS
SEE PROFILE

Published in final edited form as:
Mol Pharm. 2009 ; 6(2): 492–503. doi:10.1021/mp800174g.

Conjugation with Cationic Cell-Penetrating Peptide Increases Pulmonary Absorption of Insulin

Leena N. Patel[1], **Jeffrey Wang**[2], **Kwang-Jin Kim**[3], **Zea Borok**[3,4], **Edward Crandall**[3], and **Wei-Chiang Shen**[1,5]

[1] Department of Pharmacology and Pharmaceutical Sciences, School of Pharmacy, University of Southern California, Los Angeles, CA 90089-9121

[3] Department of Medicine, University of Southern California, Los Angeles, CA 90089-9121

[4] Department of Biochemistry and Molecular Biology[4] Will Rogers Institute Pulmonary Research Center, Keck School of Medicine, University of Southern California, Los Angeles, CA 90089-9121

[2] Department of Pharmaceutical Sciences, College of Pharmacy, Western University of Health Sciences, Pomona, CA 91766-1854

Abstract

In this study, we determined if cell-penetrating peptides (CPPs) can be used to enhance the absorption rate of insulin (INS) across the alveolar epithelial barrier. Using a heterobifuctional crosslinker, INS was conjugated to a series of cationic CPPs, including Tat peptide, oligoarginine (r9) or oligolysine (k9), via disulfide bridge to a D-isoform cysteine (c) present at the N-terminal of the peptide sequence, yielding INS-cTat, INS-cr9, and INS-ck9, respectively. SDS-PAGE and MALDI-TOF mass spectroscopy confirmed homogenous conjugates with a 1:1 ratio of INS and various CPPs. Transport of INS and INS-CPPs across primary cultured rat alveolar epithelial cell monolayers was in the order INS-cr9 > INS-cTat > INS-ck9 > INS, with 27-, 19- and 4-fold increase compared to native INS, respectively. Transport of INS-cr9 was temperature- and time-dependent. Covalent conjugation between r9 and INS, as opposed to adding unconjugated INS and r9 together into donor fluid, was necessary to enhance transport of INS. Absorption of INS-cr9 across the alveolar epithelial barrier appeared to be in part transcellular, since INS-cr9 transport in the presence of heparin and protamine was decreased by ~20%. Adsorptive transcytosis appeared to be in part responsible for INS-cr9 absorption, as INS-cr9 did not compete with free INS in binding assays for INS receptors. Finally, intratracheal instillation of INS-cr9 in diabetic rats resulted in a steady decrease in blood glucose level that was more sustained over time when compared with INS. These results suggest that oligoarginine can be used to increase the alveolar absorption rate of insulin (and potentially other macromolecules as well).

Keywords

Cell penetrating peptides; insulin; pulmonary delivery; oligoarginine

1. Introduction

The physiological and anatomic attributes of the lung make it a suitable target for systemic delivery of therapeutic molecules. The large absorptive surface area (~ 100m^2 in humans), extensive vascularization, and relatively low enzymatic activity in the distal lung may

5Corresponding author (weishen@usc.edu).

contribute to increased bioavailability of drugs delivered via the pulmonary route. However, bioavailability of high molecular weight molecules (e.g., proteins) is low compared to direct systemic delivery, partly due to the absorption barrier posed by the various epithelia lining the lungs. In particular, the lower respiratory tract that provides the large surface area for absorption consists of a tight alveolar epithelium that prevents passive permeation of macromolecules between adjoining epithelial cells. Competing pathways such as phagocytic clearance by alveolar macrophages and proteolytic degradation by macrophages and pneumocytes further limit the amount of intact peptide/protein drug available for systemic absorption [1]. Strategies employed to overcome these barriers include use of penetration enhancers 2 or incorporation of macromolecules into carrier systems such as nanospheres 3 and liposomes [4]. Another approach to increase absorption rate is to modify the macromolecule to be delivered by conjugation with biocompatible substrates or polymers. For instance, insulin has been conjugated to polyethylene glycol (PEG) of various molecular weights [5], transferrin 6, dextran [7], silk sericin peptides [8], polysialic acid 9 and deoxycholic acid [10]. These modifications all led to an increase in INS absorption rate and were shown to be effective in overcoming problems of self-aggregation and enzymatic degradation. Cell-penetrating peptides (CPPs) are short peptides of about 7–15 residues and are cationic or amphipathic in nature. Cationic CPPs are generally rich in arginine or lysine. Examples of cationic CPP include the Tat peptide derived from human immunodeficiency virus (HIV)-1 Tat protein, penetratin derived from the third helix of the Antennapedia homeodomain protein, and oligomers of arginine or lysine 11. These CPPs have been used extensively for intracellular delivery of macromolecules due to their ability to efficiently translocate across cell plasma membranes without compromising cargo bioactivity (reviewed in 12). In addition, due to their cationic nature, they bind extensively to the negatively charged ubiquitous proteoglycans found on cell surfaces and consequently have low cell specificity.

While CPPs have been widely utilized for intracellular delivery, little is known about their ability to deliver cargo (molecules attached to CPPs) across epithelial or endothelial barriers. Although permeability studies of radiolabeled Tat peptide alone show inefficient transport across MDCK or Caco-2 cells [13], CPPs tend to increase transcellular transport of macromolecules to which they are conjugated by unknown mechanisms 14, [15]. Oligoarginine conjugated to Cyclosporine A was shown to increase transport of Cyclosporine A by several fold across both the epidermal and dermal layers of skin [15]. In Caco-2 monolayers, insulin conjugated to the L-isoform of Tat peptide was reported to be transported 6–8 times more efficiently than INS [14]. Generally, both L and D isoforms of cationic CPPs increase cellular uptake of conjugated cargo. The L-isoform is prone to proteolytic degradation, whereas the D-isoform is not recognized by the degrading enzymes. Since the alveolar apical surface is known to express aminopeptidases [16] that could degrade CPPs prior to or during transport, thus decreasing the efficiency of transport, we chose to utilize the D-isoform of peptides for conjugation.

The objective of the present study was to investigate the feasibility of crosslinking INS to cationic CPPs to increase absorption of INS across the alveolar epithelium. We crosslinked INS via disulfide bridge to the D-isoform of three different cationic CPPs (i.e., Tat peptide, oligoarginine, and oligolysine) using a bifunctional crosslinker and measured transport rates of INS-CPP conjugates across primary cultured rat alveolar epithelial cell monolayers. We also explored the mechanisms for translocation of INS-CPP conjugates across the alveolar epithelium in vitro, and investigated biological activity in blood of insulin-oligoarginine, following intratracheal instillation into rats.

2. Material and Methods

2.1 Materials

Recombinant human INS was obtained from Chemicon International (Temecula, CA). ^{125}I-Tyr14-INS was obtained from Amersham Biosciences (Piscataway, NJ). Citraconic anhydride and N-succinimidyl-3-(2-pyridyldithio)propionate (SPDP) were purchased from Pierce (Rockford, IL). Prestained protein markers, Broad Range and Kaleidoscope, were purchased from BioRad (Richmond, CA). D-isoforms of oligoarginine, oligolysine, and Tat peptide (each with a D-cys residue at the N-terminal) were synthesized at 98 % purity by Genemed (San Antonio, TX).

2.2 Conjugation of INS with various CPPs

The specific conjugation at position B29 of INS with various CPPs was modified from the method reported elsewhere [17]. Briefly, insulin (20 mg/ml) was reacted with 25 μl citraconic anhydride (100 mg/ml) at pH 8 for 1.5 h, at which point most of the INS was converted to A1, B1, B29-tricitraconylinsulin. The reaction mixture was adjusted to pH 5 and incubated at room temperature for 4.5 h to partially de-block the citraconyl group at position B29. The resulting A1, B1-dicitraconyl insulin (InsP4) was purified from the mixture of several species of modified INS by HPLC with a flow rate of 1ml/min through a C4 column. The mobile phases are: solvent A (5% acetonitrile in 20 mM NH_4HCO_3) and solvent B (95% acetonitrile in 20 mM NH_4HCO_3) with 17.5 – 25% solvent B from 0 – 15 min. Collected fractions were lyophilized and stored at −20°C or used immediately. To conjugate a CPP to the amino group on B29, InsP4 (dissolved in phosphate buffer at pH 8) was first reacted with aliquots of 5 μL SPDP (50 mg/ml in DMF) every 20 min for 2 h. The reaction was monitored by intermittent HPLC analysis of the reaction mixture using the procedure described above. When more than 90% of InsP4 was modified with SPDP, InsP4-SPDP was purified by HPLC through a C18 column. Mobile phases are: solvent A (5% acetonitrile in 0.1% trifluoroacetic acid (TFA)) and solvent B (95% acetonitrile in 0.1% TFA) with 15 – 50% solvent B from 0 – 15 min. The purified InsP4-SPDP was concentrated, adjusted to pH 8 using 1N NaOH, and subsequently reacted with equimolar amounts of CPPs for 1 h to obtain INS-CPP conjugates.

2.3 Characterization and radiolabeling of conjugates

To confirm conjugation of INS to a CPP at 1:1 ratio, the products were analyzed using SDS-PAGE and MALDI-TOF mass spectroscopy. Gel electrophoresis was done under non-reducing conditions using 6.5% stacking and 15% running gels, and resultant protein bands were detected with Coomassie blue staining. Mass spectroscopic analysis of INS-CPP conjugates was performed using Krotos Kompact MALDI-TOF Mass Spectrometer (USC Proteomics Core). Approximately 10 pmol of INS-CPPs were spotted on the matrix consisting of 10 mg/ml α-cyano-4-hydroxycinnamic acid in 1% TFA/70% acetonitrile and subjected to MALDI-TOF using an Axima-CFR in the linear mode. INS and INS-CPP conjugates were labeled with ^{125}I using chloramine-T method and purified by size-exclusion chromatography using Sephadex G-25 gel matrix and stored at −20 °C until further use.

2.4 Culture of primary rat alveolar epithelial cell monolayers (RAECM) and HepG2 cell line

Isolation and purification of rat alveolar epithelial type II cells have been described in detail previously [18]. The purified type II pneumocytes on Day 0 were plated onto tissue culture-treated polycarbonate filters (12-mm (12 well) or 24-mm (6 well) Transwells, 0.4-μm pore size; Corning-Costar, Cambridge, MA) at a density of 10^6 cells/cm^2 in a culture medium (MDS) composed of a 1:1 mixture of Dulbecco's modified Eagle's medium and Ham's F-12 medium (DME-F12, Sigma, St Louis, MO) that were further supplemented with 1.25 mg/ml bovine serum albumin (BSA), 0.1 mM non-essential amino acids, 10 mM HEPES, 2 mM L-glutamine,

100 U/ml penicillin, 100 ng/ml streptomycin and 10% newborn bovine serum (NBS). RAECM were fed with fresh culture medium (containing 10 ng/ml keratinocyte growth factor (KGF)) on Days 3 and 5. All monolayers were utilized on Days 5–7 in culture. We chose to utilize RAECM grown in the presence of KGF, based on preliminary studies showing that absorption of INS-CPP conjugates was significantly greater across RAECM which are cultured in the presence rather than absence of KGF (data not shown). HepG2 cells, a human hepatoma cell line (ATCC, Rockville, MD), were cultured at 37°C in 5% CO_2, with DME supplemented with 10% fetal bovine serum, 2 mM glutamine, 50 μg/ml streptomycin and 50 U/ml penicillin.

2.5 Transport of INS and INS-CPPs across RAECM

RAECM grown on 24 mm tissue culture-treated Transwells were pre-equilibrated with MDS (without NBS) for 1 h prior to transport studies. Radiolabeled INS or INS-CPP conjugates were dosed in the apical compartment and incubated at 37°C for 2 h, after which media from the basolateral compartment were collected and subjected to the trichloroacetic acid (TCA) precipitation assay [19, 20] to determine the fraction of intact INS or INS-CPP conjugate. Radioactivity associated with the supernatant and with the pellet was measured using a gamma counter. Fraction of intact INS or INS-CPPs was estimated as the ratio between radioactivity of the pellet and the sum of radioactivities in the supernatant and pellet. For all other transport studies, RAECM grown on 12 mm tissue culture-treated Transwells were used. Apical-to-basolateral transport of intact INS- cr9 conjugate was determined at 0, 60, 120, 180, and 240 min post-dosing to construct time courses. Changes in transepithelial electrical resistance (TEER) were measured at the same time intervals as above using an epithelial volt-ohm meter (EVOM, World Precision Instruments, Sarasota, FL). TEER values at the time of dosing (i.e., t = 0 min) were designated as 100% and changes in TEER at subsequent times were calculated (relative to that at time t = 0). TEER ranged from 2.5 to 3.6 $k\Omega cm^2$ before and after the transport studies.

Temperature dependence of absorption of INS-cr9 across RAECM was studied by pre-equilibrating RAECM at 37° or 4°C with MDS (without NBS) for 1 h prior to dosing with INS-cr9 conjugate into apical fluid. Effects of positive charge-bearing molecules (e.g., heparin or protamine, 1 μM each), metabolic inhibitors (10 mM NaN_3 or 6 mM 2-deoxyglucose), and endocytosis inhibitors (10 mM NH_4Cl, 30 μM monensin, 33 μM nocodazole, 30 μM chlorpromazine or 0.1 μg/ml cytochalasin D) were determined by pre-incubating an appropriate agent for 1 h in the apical compartment of RAECM, followed by determination of INS-cr9 transport in the apical-to-basolateral direction for 2 h at 37°C with or without the agent in the apical fluid.

2.6 In vitro biological assay by estimating INS and INS-cr9 that bind insulin receptors expressed in HepG2 cells

HepG2 cells were seeded onto surfaces of 24-well cluster plates at a density of 4×10^5 cells/well. Confluent HepG2 monolayers (HGM) obtained on Day 3 of seeding were utilized for ligand binding assay. HGM were washed twice with PBS before equilibrating with DME containing 0.1% BSA for 30 min. A ligand solution containing 50 pM ^{125}I-Tyr14-INS alone or containing in addition various concentrations (1 pM, 10 pM, 100 pM, 1 nM, 10 nM and 100 nM) of unlabeled INS or INS-cr9 were prepared in DME containing 0.1% BSA. Competitive inhibition by unlabeled INS or INS-cr9 for binding of ^{125}I-Tyr14-INS to insulin receptors at steady state was determined by incubating HGM with an appropriate ligand solution for 2 h at 4 °C, after which the unbound ^{125}I-Tyr14 INS was removed by washing with PBS 3 times. Washed HGM were then solubilized in 0.1% NaOH and aliquots of solubilized monolayers were assayed for radioactivity using a gamma counter. Concentrations of solubilized HGM were determined by the bicinchoninic acid (BCA) assay (Pierce). Binding data were analyzed for estimation of apparent binding constant for radiolabeled INS for insulin receptors

(inhibition constant (IC50) of unlabeled INS or INS-cr9 as an index for competitive binding to insulin receptors).

2.7 Pharmacological activity of INS-cr9 in diabetic rats

2.7.1 Induction of diabetes in rats—The animal studies described in this section were approved by the Institutional Animal Care and Use Committee of the University of Southern California, and the procedures were conducted according to the guide for the Care and Use of Laboratory Animals (National Research Council, 1996). Sprague-Dawley male rats (10 weeks and 250–280 g) obtained from Harlan (Indianapolis, IN) were housed under standard laboratory conditions (i.e., relative humidity of 65 ± 2%, temperature of 23 ± 2°C, and 12-hr light-dark cycle). Rats were fed with a standard rodent pellet diet and tap water ad libitum when not subjected to experimental procedures. Rats were allowed to acclimatize for 3 days prior to starting the pharmacologic experiments. Rats were fasted overnight and fasting glucose levels at baseline determined before intraperitoneal injection of freshly prepared streptozotocin (STZ, 60 mg/kg in pH 4.5 acetate buffer) to induce diabetes. Five days after STZ-treatment, rats with a fasting plasma glucose level of > 400 mg/dl were selected for further studies.

2.7.2 Intratracheal instillation of INS-cr9, INS, and control (i.e., saline) solution into rats

Selected diabetic rats were fasted overnight and divided into 3 groups with 4 rats per group for control, INS, or INS-cr9. The animals were anesthetized by intraperitoneal injection of a mixture of xylazine (10 mg/kg) and ketamine (90 mg/kg). Dosing solution (100 μl of INS, INS-cr9 or PBS) was administered intratracheally 5 minutes after anesthesia using 1A–1B MicroSprayer (Penn Century, Philadelphia, PA) attached to a 1 ml syringe. During administration, the animal was held in a lateral position on a restrainer and the tongue pulled aside using blunt forceps to expose the larynx. The microsprayer was then guided to the glottis region by illumination with a fiberoptic otoscope and gently pushed further into the trachea where the dosing solution was sprayed near the bifurcation of trachea to two main bronchi. The animal was held in a vertical position for 1 min after intratracheal administration of the dosing solution, then placed on a blanket and allowed to recover. A drop of blood (~ 20 μl) from the tail vein was withdrawn at predetermined time points (up to 7 h) to measure its glucose level using the ONE TOUCH ULTRA blood glucose monitoring system (Lifescan, Milpitas, CA). Glucose levels in blood were expressed as percentage of initial glucose levels (i.e., that measured prior to anesthesia was 100%).

2.8 Statistical Analysis

For comparison of two groups, paired or unpaired Student's *t*-tests were used to determine statistical significance. One way analyses of variance (ANOVA) with *post hoc* Bonferroni's tests were used for comparisons of 3 or more groups. A level of $p < 0.05$ was considered statistically significant.

3. Results

3.1 Conjugation of INS to CPPs and characterization of INS-cr9, INS-ck9 and INS-cTat conjugates

Conjugation of cr9, cTat or ck9 to INS was achieved by using a heterobifunctional crosslinker, SPDP, that is reactive to -NH_2 and -SH groups (Table I). Specific conjugation to lysine moiety in the B-chain of INS was achieved by blocking all three amino groups on INS with citraconyl anhydride, followed by partial de-blocking of the citraconyl group on B-Lys 29 through pH manipulation (Figure 1). To obtain a homogeneous conjugate, purification steps using reversed-phase HPLC for every intermediate were employed. The final products were eluted

at retention times of 11.60, 11.76 and 11.90 min for INS-cr9, INS-cTat and INS-ck9, respectively.

SDS-PAGE was used to determine changes in molecular weights of INS-CPP conjugates in comparison with INS. The gel was run in the absence of any reducing agent in order to protect a disulfide linkage between INS and various CPPs. In Figure 2A, lane 1 shows the pattern of broad range protein markers with the lowest molecular weight of 7.6 kDa. Lane 2 shows INS, whereas lane 3 and 4 show the INS-cr9 band with a marginal upward shift, representing a higher molecular weight, as compared to INS. Lanes 5–8 are part of a separate gel showing the pattern of prestained Kaleidoscope markers, INS, INS- cTat and INS-ck9, respectively. Prominent bands for INS-cTat and INS-ck9 are seen as being shifted upward from the INS band, as expected.

The conjugates were further analyzed by MALDI-TOF mass spectrometry to determine the exact molecular weight and to confirm that monosubstituted conjugates were obtained. Figure 2B-(i) shows the spectrum of INS-cr9 with observed molecular mass of 7466.29 (expected average molecular weight = 7421). A difference of ~ 45 Da between the observed and expected molecular weight could likely be due to the addition of 2 sodium ions on the two carboxyl terminals of INS chains A and B. Figure 2B-(ii) represents the mass spectra of INS-cTat with observed molecular mass of 2399.74 (since expected average molecular weight is 7338 for INS-cTat, the low molecular mass of 2399.74 is most likely due to a mass charge ratio of 1:3). Figure 2B-(iii) shows INS-ck9 (expected molecular weight = 7169) with an observed molecular mass of 7165.01.

3.2 Higher transport of INS-cr9 compared to INS-cTat and INS-ck9 across RAECM

To compare the transport efficiency across RAECM, the radiolabeled conjugates and INS were dosed apically at 37°C for 2 h. Figure 3 shows the fraction of intact INS and INS-CPP conjugates as a percentage of the dose transported into basolateral fluid over 2 h. Compared to INS, all three INS-CPP conjugates showed significantly higher transport. The magnitude of increase was 27-, 19- and 4-fold compared to INS with INS-cr9, INS-ck9 and INS-cTat, respectively.

3.3 Time course studies of INS, INS-cr9, and a 1:1 mixture of INS and cr9

Transport of 5 μg/ml of INS, INS-cr9 (with INS equivalent of 5 μg/ml), or a 1:1 mixture of INS and cr9 (5 μg/ml and 1.3 μg/ml, respectively) following apical dosing was compared over 4 h (Figure 4A). Transport of INS-cr9 had a lag period of 1 h, followed by a linear increase for the next 3 h. A 1:1 mixture of INS and cr9 did not show such an increase in transport over time, underscoring the importance of covalent conjugation of oligoarginine to INS for enhancing transalveolar epithelial absorption.

3.4 Effect of INS-cr9 on TEER of RAECM

TEER is commonly used as a measure of cell monolayer integrity and is negatively correlated with paracellular permeability of molecules across the monolayer [21, 22]. Figure 4B shows the effect of INS-cr9 on TEER of RAECM during 4 h transport studies. The initial TEER of monolayers utilized was 3.3 ± 0.6 kΩcm^2 (n = 36). INS-cr9 caused a slow decline in TEER by ~19% over 4 h. By contrast, TEER observed with INS alone or a 1:1 mixture of INS and cr9 was not significantly different from that of control (t = 0).

3.5 Effects of temperature and charge-bearing molecules on INS-cr9 absorption across RAECM

To determine the effect of temperature, transalveolar epithelial absorption of INS-cr9 measured at 37°C was compared to that measured at 4°C. Figure 5A shows that transport of intact INS-cr9 decreased by ~79% at 4°C compared to that at 37°C, suggesting that the INS-cr9 conjugate may be transported primarily via transcellular (but not paracellular) pathway(s). To determine if the presence of negatively- or positively-charged molecules could affect the transport of INS-cr9 which is highly positively- charged, RAECM were pre-treated with 1 μM of either heparin (negatively-charged) or protamine (positively-charged). Figure 5B shows the effect of heparin and protamine on the absorption of INS-cr9 across RAECM. In the presence of heparin, a 19.4 ± 4.5 % decrease in transport was observed, whereas a decrease of 23.2 ± 8.6 % with protamine was seen, suggesting that INS-cr9 absorption is mildly influenced by charge-charge interactions between positive charges on INS-cr9 and negative charge bearing cell plasma membrane components (e.g., proteoglycans).

3.6 Effect of biochemical modulators on transalveolar absorption of INS-cr9

To further probe transcellular mechanisms by which INS-cr9 is transported across RAECM, various inhibitors of endocytosis and cell energy production were tested (Table II). In the presence of agents that are known to deplete cellular energy (e.g., NaN_3 and 2-deoxyglucose), a reduction of 15 % in INS-cr9 absorption was observed compared to control ($p < 0.05$). By contrast, no statistically significant decreases in INS-cr9 absorption were observed in the presence of various endocytosis inhibitors (e.g., ammonium chloride, monensin and chlorpromazine). By contrast, a 40% increase in INS-cr9 absorption was seen with a microtubule inhibitor, nocodazole, which led to a 70% decrease in cell integrity as measured by TEER.

3.7 Lack of competition by INS-cr9 in binding assay of insulin receptors

In vitro biological activity of INS-cr9 was tested by assays designed to determine competition afforded by unlabeled insulins against labeled insulin binding its cognizant receptors expressed in HepG2 cells[10]. ^{125}I-Tyr14-Insulin, which was labeled at Tyr14 of the B-chain, was used as the radioligand. Preliminary studies indicated that saturation of ^{125}I-Tyr14-Insulin occurs with an apparent Kd of 125 ± 29 pM (data not shown). Figure 6A shows competition profiles for insulin receptor binding when increasing concentrations of unlabeled INS or INS-cr9 up to 100 nM were used. As can be seen, unlabeled INS competed binding of labeled INS to insulin receptors with an IC_{50} of 1.2 (± 0.4) nM, whereas unlabeled INS-cr9 in increasing concentrations did not compete at all with labeled INS binding its receptors, suggesting that the observed large rates of INS-cr9 absorption across RAECM may not be related to transcytosis mediated by INS receptors.

3.8 Higher and prolonged effect of INS-cr9 after spray instillation

The time course of blood glucose level after intratracheally spraying INS-cr9 into lungs of diabetic rats is shown in Figure 6B. Instillation of INS-cr9 led to a small increase (~20%) in glucose levels up to 60 min post-administration, after which a gradual decline of blood glucose levels down to below 20% of the initial glucose level was observed between 5 to 7 h. A complete response curve was not obtainable in this study due to the long period of fast in this experiment. Administration of INS resulted in a 20% decrease in blood glucose levels at 120 min, and continued to decrease over the next 180 min to ~ 40% of those at t =0. By contrast, an equal volume of PBS did not show any significant effect on blood glucose level over similar time periods.

4. Discussion

In this study, the potential of cationic cell-penetrating peptides (i.e., Tat, oligolysine and oligoarginine) for increasing pulmonary delivery of INS was demonstrated. Covalent conjugation of CPP to INS resulted in significantly higher absorption rates across RAECM of all three conjugates (i.e., INS-cr9, INS-cTat, and INS-ck9) tested compared to that observed for INS. Furthermore, alveolar absorption of INS- cr9, the most efficient conjugate of the three, was determined to be time- and temperature- dependent, with no considerable effect on RAECM TEER.

By site-specific linkage using a heterobifunctional cross-linker, conjugates with a 1:1 ratio of INS and CPP were obtained. Insulin contains three amino groups: two N-terminal α-amino groups; Gly at A1 (Gly-A1, pKa of 8.4) and Phe at B1 (Phe-B1, pKa of 7.1) chain and one ε-amino group at Lys 29 at B-chain (Lys-B29, pKa > 9.8). Due to its much higher pKa than corresponding pKa of Gly-A1 and Phe-B1, the reactivity of Lys-B29 is greater than Gly-A1 and Phe-B1 at higher pH, which allows us to covalently conjugate other molecules specifically to Lys-B29 [5, 10, 23]. From our preliminary data and literature survey, this conjugation method appears to result in heterogeneous conjugates which are difficult to separate [24]. Furthermore, heteroconjugates exhibit different biological activities due to batch-to-batch variations. We therefore (1) utilized a multistep process in which a protecting agent, citraconyl anhydride, was used to reversibly block the a-amino groups to increase the reactivity of Lys-B29 and (2) purified each intermediate derivative using reversed-phase HPLC to obtain homogeneous conjugates. The homogeneity of the conjugates is evidenced by a single band on the SDS-PAGE gel and corroborated by the resultant spectra of MALDI-TOF MS.

Tat peptide is the most widely studied cationic CPP. Structure-activity studies of the various CPPs show that arginine plays an important role in internalization of CPP into various cells [25]. In addition, the cellular uptake efficiency is also dependent on other factors such as overall charge, length and isomeric form of the peptide [26]. Because L-isoform peptides are metabolically unstable or easily digested by peptidases [27] and alveolar epithelial cells are known to exhibit high aminopeptidase activity [16, 28], we chose to use the D-isoform of the peptides for conjugation. Several studies have compared the cellular uptake of different cationic CPPs alone or those covalently conjugated to various macromolecules [12, 29]. The results shown in this study are the first to our knowledge, which compare transcellular transport of different cationic CPPs conjugated to a macromolecule (i.e., insulin). Our data show that the transport efficiency of the INS-CPP conjugates and INS was in the order INS-cr9 > INS-cTat > INS-ck9 > INS. These data suggest that INS-CPP can increase cellular uptake through permeation of the apical layer and enhance permeation of cargo through the basolateral layer. The rank order in transport efficiency is consistent with uptake efficiency in other cell lines (e.g., Chinese hamster ovary (CHO) cells and Jurkat cells) [26, 30]. Compared to INS-cTat and INS-ck9, INS-cr9 showed a more pronounced increase (27-fold) in absorption across RAECM. Thus, we chose INS-cr9 for further investigations for transport mechanisms and in vivo studies of pulmonary delivery.

It is generally accepted that covalent linkage between a cationic CPP and the cargo of interest is required to enhance cellular uptake. Whether the covalent bond is reversible or not depends on the nature of the cargo. Morishita *et al* [31] recently showed that in situ absorption of INS across rat ileum could be enhanced by physically mixing oligoarginine with INS and that covalent conjugation was not necessary. By contrast, our studies with INS and cr9 in RAECM show that an increase in INS transport across RAECM was not apparent when a mixture of INS and oligoarginine was used. Possible reasons for this discrepancy include differences in the concentrations used and the type of cells and tissues utilized in each study. Oligoarginine concentration in our transport study was in the μM range, whereas Morishita *et al* 31 used

oligoarginine in the mM range. At such a high concentration, it is likely that portions transported via paracellular pathways may be increased commensurately. In fact, polyarginine with high molecular weight (~ 42.4 kDa) was shown to decrease TEER of nasal epithelium and increase paracellular transport of hydrophilic macromolecules via disruption of tight junctions [32]. Similar reduction in TEER is noted with cationic polymers like poly-L-lysine (MW ~ 20 kDa) and chitosan (MW 31 kDa) in MDCK and Caco-2 cells, respectively 33, 34. In our study, TEER did not decrease when RAECM was apically incubated with a mixture of cr9 and INS, possibly due to the low concentration. Moreover, concentrations of up to 100 μM of oligoarginine did not significantly affect TEER of RAECM (data not shown). When INS-cr9 was added apically, there was a small drop in TEER which did not decrease below 80% of control and hence was not likely to have affected significantly paracellular transport of hydrophilic solutes (including INS-cr9 conjugates). The decrease in TEER of RAECM seen with INS-cr9, but not seen when INS is added to apical fluid together with cr9, leads us to speculate that INS-cr9 conjugates interact directly or indirectly with extracellular and/or intracellular component(s) that might lead to modulation of tight junctional properties.

Lowering temperature from 37°C to 4°C caused ~80% decrease in absorption of INS-cr9 across RAECM. By contrast, decreasing temperature to 4°C results in approximately 37% and 40% inhibition of paracellular transport of INS 19 and FITC-dextran [35] across RAECM. A much greater decrease in absorption observed at 4°C for INS-cr9 conjugates indicates the involvement of process(es) other than passive leak through paracellular pathways. Moreover, in the presence of inhibitors of cell energy generation (NaN3 and 2-deoxyglucose), a statistically significant reduction in INS-cr9 absorption was observed, suggesting involvement of cell energy-dependent process(es). Interestingly, transcellular pathways for much larger positively charged polystyrene nanoparticles (20 and 120 nm diameters) were suggested based on results showing >85% inhibition in nanoparticle trafficking across RAECM at 4°C compared to 37°C [36].

The mechanisms by which CPP translocate across cell membranes are not well understood. Involvement of different types of endocytosis has been implicated, and the nature of cargo, cell type and experimental methods all seem to play important roles in determining the extent of CPP internalization [12]. In general, transcytosis can occur as a result of both non-specific (i.e., adsorptive and fluid-phase) and specific (i.e., receptor-mediated) endocytosis, involving a number of complex steps (including vesicle formation from cell plasma membranes and vesicle fusion to other intracellular vesicles) and different cellular machinery including cytoskeletal networks. Our findings on the effects of heparin and protamine indicate that absorption of INS-cr9 may occur in part via adsorptive endocytosis (and subsequent transcytosis). Heparin is polyanionic in nature and is shown to inhibit adsorptive-mediated transcytosis of polylysine-tyramine conjugate in MDCK cells [37], while protamine was used to inhibit adsorptive transcytosis of cationic peptides in Caco-2 cells 38. Heparin would therefore neutralize the positive charge of INS-cr9, whereas a polycation protamine would compete with INS-cr9 for the anionic binding sites on the cell surface. Both inhibitors showed a modest yet statistically significant decrease in INS-cr9 absorption, suggesting that translocation of INS-CPP conjugates across RAECM may be in small part mediated by adsorptive transcytosis.

Ammonium chloride 39 and monensin [40] are known to disrupt transcytosis and secretory pathways (e.g., intracellular organelles whose pH is acidic) by alkalinization and interference with vesicular Na^+/H^+ exchange, respectively. However, these two agents did not affect transport of INS-cr9 across RAECM. Moreover, chlorpromazine [41], an inhibitor of clathrin-mediated endocytosis, did not show any statistically significant effect, suggesting limited involvement of clathrin-mediated endocytosis/transcytosis in INS-cr9 absorption across RAECM. Unexpectedly, an increase rather than decrease in INS-cr9 absorption across RAECM was observed in the presence of microtubule inhibitor, nocodoazole. Microtubules

are important cytoplasmic elements that facilitate the movement of vesicles and substrates in the cytoplasm. Inhibition of microtubule formation is thus expected to limit vesicular transcytosis, if any. It should be pointed out that the drastic drop in TEER observed with nocodazole treatment is consistent with paracellular leakage of INS-cr9. This latter explanation can be further supported by the findings of Birukova *et al*[42], who showed that nocodazole leads to barrier dysfunction of endothelial cell monolayers by cell retraction and paracellular gap formation.

In vitro biological activity of INS-cr9 was tested by competition assay for binding of INS to its receptors using a HepG2 cell line. Since the site of modification on INS, Lys-B29, is peripheral to the region essential for binding of INS to its receptors [43], we expected that INS-cr9 would bind to INS receptors. To our surprise, INS-cr9 did not seem to compete for binding to INS receptors for a concentration of up to 100 nM. Shortening of the B-chain of INS by five amino acids increases the receptor binding affinity of INS due to conformational changes that further expose the N-terminal residues of the A-chain [44]. Conjugation with hydrophilic polymers like polyethylene glycol [5, 45] to Lys-B29 does not interfere with receptor binding. On the other hand, Detemir, an INS analogue with a C14 fatty acid attached at the same position, led to ~50% reduction in receptor binding, due perhaps to hydrophobic interactions with the neighboring aromatic amino acids [46]. We speculate that the lack of binding of INS-cr9 to INS receptors may be due to unfavorable conformational changes caused by the charge repulsion of positively charged cr9 or may be due to steric hindrances caused by the increased hydrodynamic size of the resultant conjugate.

Activity in diabetic rats in vivo was evidenced by a drop in blood glucose levels following intratracheal instillation of INS-cr9. Compared to the effects of INS on blood glucose levels, INS-cr9 showed better pharmacodynamic activity that was sustained over time and maintained blood glucose below 20% of the baseline level between 5 to 7 h after intratracheal administration (Fig. 6B). This latter finding suggests that the disulfide bond between cysteine of cr9 and the linker attached to Lys-B29 is reduced in vivo to generate biologically active INS, although the molecular mechanisms of this reductive reaction remain to be determined.

The absolute bioavailability of insulin conjugate was not measured in this study. To accomplish that, we are currently developing analytical assay for both the conjugate and the regenerated insulin. Nevertheless, results from the in vivo pharmacodynamic study described herein (Fig. 6B) clearly indicate that the bioavailability of the conjugate is greater than insulin itself in pulmonary absorption.

In summary, we have shown that conjugation of INS with CPPs can enhance absorption of INS across the alveolar epithelial barrier in vitro as well as in vivo. Of the CPPs studied, oligoarginine turns out to be a more efficient carrier for absorption of INS across RAECM than Tat or oligolysine. The oligoarginine-INS conjugate (INS-cr9) may be in small part transported by adsorptive transcytosis pathways, with other yet unknown transcellular mechanisms likely to be involved. INS-cr9 does not bind to INS receptors in vitro, whereas upon pulmonary delivery it exerts biological activity presumably due to separation of INS-cr9 from INS via reduction of disulfide bonds. Cationic cell- penetrating peptides can potentially be used to increase the absorption rate of other protein and peptide drugs across the alveolar epithelial barrier.

Acknowledgments

We would like to thank Mrs. Daisy Shen for technical assistance with the in vivo studies and Dr. Yi Ming Chiang for help with the HPLC system. This study was supported in part by the Hastings Foundation and National Institutes of Health research grants GM070777, HL038578, HL038621, HL038658, HL062569 and HL064635. ZB is Ralph

Edgington Chair in Medicine. EDC is Kenneth T. Norris Chair and Hastings Professor of Medicine. WCS is John A. Biles Professor of Pharmaceutical Sciences.

References

1. Sakagami M. In vivo, in vitro and ex vivo models to assess pulmonary absorption and disposition of inhaled therapeutics for systemic delivery. Adv Drug Deliv Rev 2006;58(9–10):1030–60. [PubMed: 17010473]
2. Kumar TM, Misra A. Influence of absorption promoters on pulmonary insulin bioactivity. AAPS PharmSciTech 2003;4(2):E15. [PubMed: 12916897]
3. Kawashima Y, Yamamoto H, Takeuchi H, Fujioka S, Hino T. Pulmonary delivery of insulin with nebulized DL-lactide/glycolide copolymer (PLGA) nanospheres to prolong hypoglycemic effect. J Control Release 1999;62(1–2):279–87. [PubMed: 10518661]
4. Huang YY, Wang CH. Pulmonary delivery of insulin by liposomal carriers. J Control Release 2006;113 (1):9–14. [PubMed: 16730838]
5. Hinds K, Koh JJ, Joss L, Liu F, Baudys M, Kim SW. Synthesis and characterization of poly(ethylene glycol)-insulin conjugates. Bioconjug Chem 2000;11(2):195–201. [PubMed: 10725096]
6. Xia CQ, Wang J, Shen WC. Hypoglycemic effect of insulin-transferrin conjugate in streptozotocin-induced diabetic rats. J Pharmacol Exp Ther 2000;295(2):594–600. [PubMed: 11046093]
7. Baudys M, Letourneur D, Liu F, Mix D, Jozefonvicz J, Kim SW. Extending insulin action in vivo by conjugation to carboxymethyl dextran. Bioconjug Chem 1998;9(2):176–83. [PubMed: 9548532]
8. Zhang YQ, Ma Y, Xia YY, Shen WD, Mao JP, Xue RY. Silk sericin-insulin bioconjugates: synthesis, characterization and biological activity. J Control Release 2006;115(3):307–15. [PubMed: 17034892]
9. Jain S, Hreczuk-Hirst DH, McCormack B, Mital M, Epenetos A, Laing P, Gregoriadis G. Polysialylated insulin: synthesis, characterization and biological activity in vivo. Biochim Biophys Acta 2003;1622 (1):42–9. [PubMed: 12829260]
10. Lee S, Kim K, Kumar TS, Lee J, Kim SK, Lee DY, Lee YK, Byun Y. Synthesis and biological properties of insulin-deoxycholic acid chemical conjugates. Bioconjug Chem 2005;16(3):615–20. [PubMed: 15898729]
11. Murriel CL, Dowdy SF. Influence of protein transduction domains on intracellular delivery of macromolecules. Expert Opin Drug Deliv 2006;3(6):739–46. [PubMed: 17076596]
12. Patel LN, Zaro JL, Shen WC. Cell penetrating peptides: intracellular pathways and pharmaceutical perspectives. Pharm Res 2007;24(11):1977–92. [PubMed: 17443399]
13. Violini S, Sharma V, Prior JL, Dyszlewski M, Piwnica-Worms D. Evidence for a plasma membrane-mediated permeability barrier to Tat basic domain in well-differentiated epithelial cells: lack of correlation with heparan sulfate. Biochemistry 2002;41(42):12652–61. [PubMed: 12379107]
14. Liang JF, Yang VC. Insulin-cell penetrating peptide hybrids with improved intestinal absorption efficiency. Biochem Biophys Res Commun 2005;335(3):734–8. [PubMed: 16115469]
15. Rothbard JB, Garlington S, Lin Q, Kirschberg T, Kreider E, McGrane PL, Wender PA, Khavari PA. Conjugation of arginine oligomers to cyclosporin A facilitates topical delivery and inhibition of inflammation. Nat Med 2000;6(11):1253–7. [PubMed: 11062537]
16. Yamahara H, Morimoto K, Lee VH, Kim KJ. Effects of protease inhibitors on vasopressin transport across rat alveolar epithelial cell monolayers. Pharm Res 1994;11(11):1617–22. [PubMed: 7870680]
17. Naithani VK, Gattner HG. Preparation and properties of citraconylinsulins. Hoppe Seylers Z Physiol Chem 1982;363(12):1443–8. [PubMed: 6761261]
18. Cheek JM, Kim KJ, Crandall ED. Tight monolayers of rat alveolar epithelial cells: bioelectric properties and active sodium transport. Am J Physiol 1989;256(3 Pt 1):C688–93. [PubMed: 2923201]
19. Bahhady R, Kim KJ, Borok Z, Crandall ED, Shen WC. Characterization of protein factor(s) in rat bronchoalveolar lavage fluid that enhance insulin transport via transcytosis across primary rat alveolar epithelial cell monolayers. Eur J Pharm Biopharm. 2008
20. Bur M, Huwer H, Lehr CM, Hagen N, Guldbrandt M, Kim KJ, Ehrhardt C. Assessment of transport rates of proteins and peptides across primary human alveolar epithelial cell monolayers. Eur J Pharm Sci 2006;28(3):196–203. [PubMed: 16533597]

21. Dodoo AN, Bansal S, Barlow DJ, Bennet FC, Hider RC, Lansley AB, Lawrence MJ, Marriott C. Systematic investigations of the influence of molecular structure on the transport of peptides across cultured alveolar cell monolayers. Pharm Res 2000;17(1):7–14. [PubMed: 10714601]
22. Dodoo AN, Bansal SS, Barlow DJ, Bennet F, Hider RC, Lansley AB, Lawrence MJ, Marriott C. Use of alveolar cell monolayers of varying electrical resistance to measure pulmonary peptide transport. J Pharm Sci 2000;89(2):223–31. [PubMed: 10688751]
23. Gao J, Mrksich M, Gomez FA, Whitesides GM. Using capillary electrophoresis to follow the acetylation of the amino groups of insulin and to estimate their basicities. Anal Chem 1995;67(18): 3093–100. [PubMed: 8686881]
24. Calceti P, Salmaso S, Walker G, Bernkop-Schnurch A. Development and in vivo evaluation of an oral insulin-PEG delivery system. Eur J Pharm Sci 2004;22(4):315–23. [PubMed: 15196588]
25. Wender PA, Mitchell DJ, Pattabiraman K, Pelkey ET, Steinman L, Rothbard JB. The design, synthesis, and evaluation of molecules that enable or enhance cellular uptake: peptoid molecular transporters. Proc Natl Acad Sci U S A 2000;97(24):13003–8. [PubMed: 11087855]
26. Mitchell DJ, Kim DT, Steinman L, Fathman CG, Rothbard JB. Polyarginine enters cells more efficiently than other polycationic homopolymers. J Pept Res 2000;56(5):318–25. [PubMed: 11095185]
27. Trehin R, Nielsen HM, Jahnke HG, Krauss U, Beck-Sickinger AG, Merkle HP. Metabolic cleavage of cell-penetrating peptides in contact with epithelial models: human calcitonin (hCT)-derived peptides, Tat(47–57) and penetratin(43–58). Biochem J 2004;382(Pt 3):945–56. [PubMed: 15193145]
28. Forbes B, Wilson CG, Gumbleton M. Temporal dependence of ectopeptidase expression in alveolar epithelial cell culture: implications for study of peptide absorption. Int J Pharm 1999;180(2):225–34. [PubMed: 10370193]
29. Dietz GP, Bahr M. Delivery of bioactive molecules into the cell: the Trojan horse approach. Mol Cell Neurosci 2004;27(2):85–131. [PubMed: 15485768]
30. Zaro JL, Shen WC. Quantitative comparison of membrane transduction and endocytosis of oligopeptides. Biochem Biophys Res Commun 2003;307(2):241–7. [PubMed: 12859946]
31. Morishita M, Kamei N, Ehara J, Isowa K, Takayama K. A novel approach using functional peptides for efficient intestinal absorption of insulin. J Control Release 2007;118(2):177–84. [PubMed: 17270307]
32. Ohtake K, Natsume H, Ueda H, Morimoto Y. Analysis of transient and reversible effects of poly-L-arginine on the in vivo nasal absorption of FITC-dextran in rats. J Control Release 2002;82(2–3): 263–75. [PubMed: 12175742]
33. McEwan GT, Jepson MA, Hirst BH, Simmons NL. Polycation-induced enhancement of epithelial paracellular permeability is independent of tight junctional characteristics. Biochim Biophys Acta 1993;1148(1):51–60. [PubMed: 8499468]
34. Schipper NG, Olsson S, Hoogstraate JA, deBoer AG, Varum KM, Artursson P. Chitosans as absorption enhancers for poorly absorbable drugs 2: mechanism of absorption enhancement. Pharm Res 1997;14(7):923–9. [PubMed: 9244151]
35. Matsukawa Y, Lee VH, Crandall ED, Kim KJ. Size-dependent dextran transport across rat alveolar epithelial cell monolayers. J Pharm Sci 1997;86(3):305–9. [PubMed: 9050797]
36. Yacobi NR, Demaio L, Xie J, Hamm-Alvarez SF, Borok Z, Kim KJ, Crandall ED. Polystyrene nanoparticle trafficking across alveolar epithelium. Nanomedicine. 2008
37. Taub ME, Wan J, Shen WC. Transepithelial transport of tyramine across filter-grown MDCK cells via a poly(D-lysine) carrier. Pharm Res 1994;11(9):1250–6. [PubMed: 7816752]
38. Sai Y, Kajita M, Tamai I, Wakama J, Wakamiya T, Tsuji A. Adsorptive-mediated transcytosis of a synthetic basic peptide, 001-C8 in Caco-2 cells. Pharm Res 1998;15(8):1305–9. [PubMed: 9706066]
39. Seglen PO, Grinde B, Solheim AE. Inhibition of the lysosomal pathway of protein degradation in isolated rat hepatocytes by ammonia, methylamine, chloroquine and leupeptin. Eur J Biochem 1979;95(2):215–25. [PubMed: 456353]
40. Deffebach ME, Bryan CJ, Hoy CM. Protein movement across cultured guinea pig trachea: specificity and effect of transcytosis inhibitors. Am J Physiol 1996;271(5 Pt 1):L744–52. [PubMed: 8944717]

41. Huang M, Ma Z, Khor E, Lim LY. Uptake of FITC-chitosan nanoparticles by A549 cells. Pharm Res 2002;19(10):1488–94. [PubMed: 12425466]

42. Birukova AA, Smurova K, Birukov KG, Usatyuk P, Liu F, Kaibuchi K, Ricks-Cord A, Natarajan V, Alieva I, Garcia JG, Verin AD. Microtubule disassembly induces cytoskeletal remodeling and lung vascular barrier dysfunction: role of Rho-dependent mechanisms. J Cell Physiol 2004;201(1):55–70. [PubMed: 15281089]

43. Gammeltoft S. Insulin receptors: binding kinetics and structure-function relationship of insulin. Physiol Rev 1984;64(4):1321–78. [PubMed: 6387730]

44. Zakova L, Barth T, Jiracek J, Barthova J, Zorad S. Shortened insulin analogues: marked changes in biological activity resulting from replacement of TyrB26 and N-methylation of peptide bonds in the C-terminus of the B-chain. Biochemistry 2004;43(8):2323–31. [PubMed: 14979729]

45. Hinds KD, Kim SW. Effects of PEG conjugation on insulin properties. Adv Drug Deliv Rev 2002;54 (4):505–30. [PubMed: 12052712]

46. Kurtzhals P, Schaffer L, Sorensen A, Kristensen C, Jonassen I, Schmid C, Trub T. Correlations of receptor binding and metabolic and mitogenic potencies of insulin analogs designed for clinical use. Diabetes 2000;49(6):999–1005. [PubMed: 10866053]

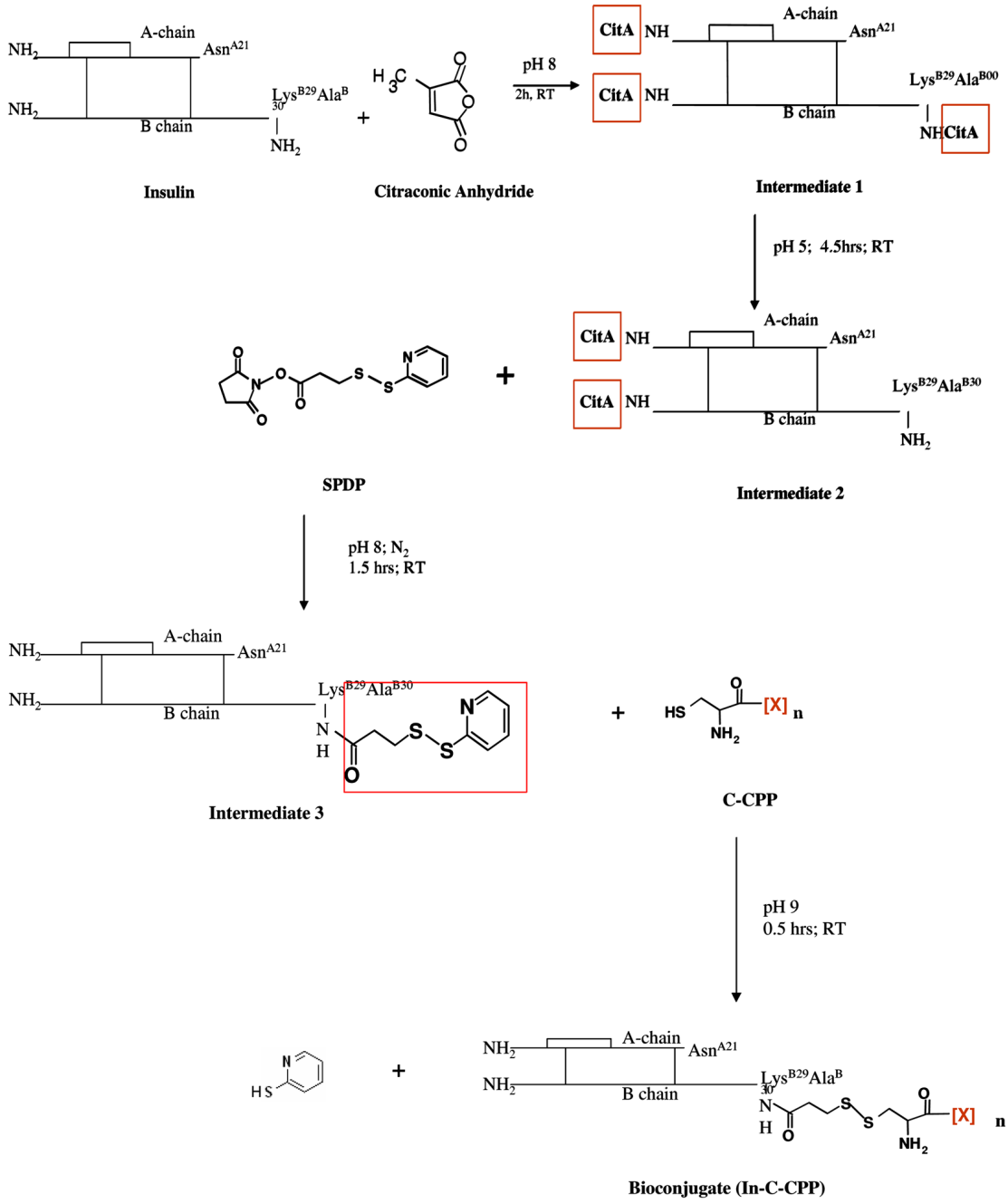

Figure 1.

Schematic presentation of INS conjugation with various cell-penetrating peptides (cr9, cTat, and ck9) using disulfide chemistry. CitA is citraconic acid, c-CPP is cysteine (d-isoform)-CPP, $[X]_n$ refers to r9, k9, or Tat peptide, and RT = room temperature.

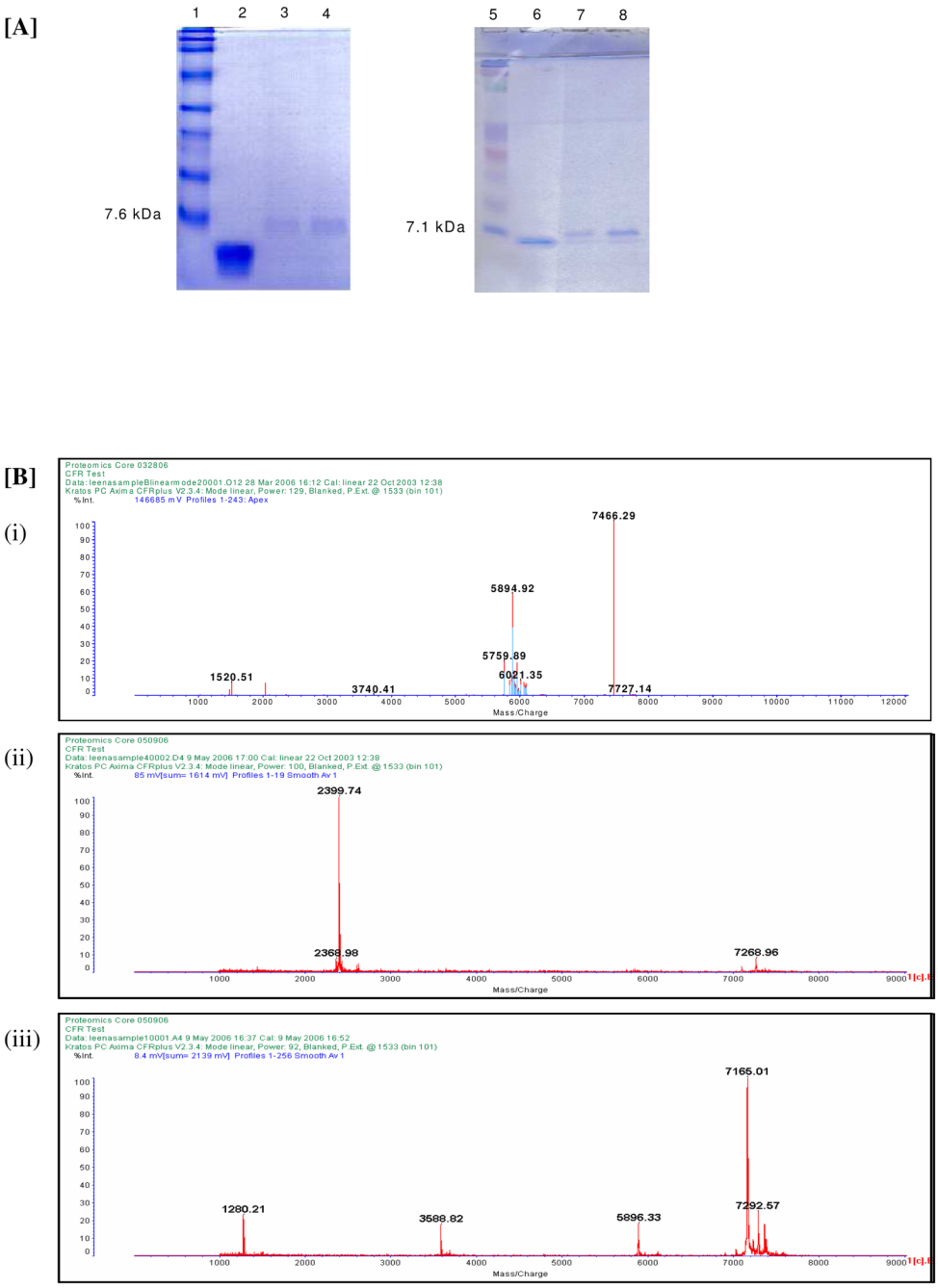

Figure 2.

[A] SDS-PAGE analysis. Lane 1 = broad range marker, lanes 2 and 6 = INS, lanes 3 and 4 = duplicates of INS-cr9, lane 5 = Precision Plus prestained marker, lane 7 = INS-cTat and lane 8 = INS-ck9. **[B]** MALDI-TOF mass spectra of (i) INS-cr9, (ii) INS-cTat and (iii) INS-ck9.

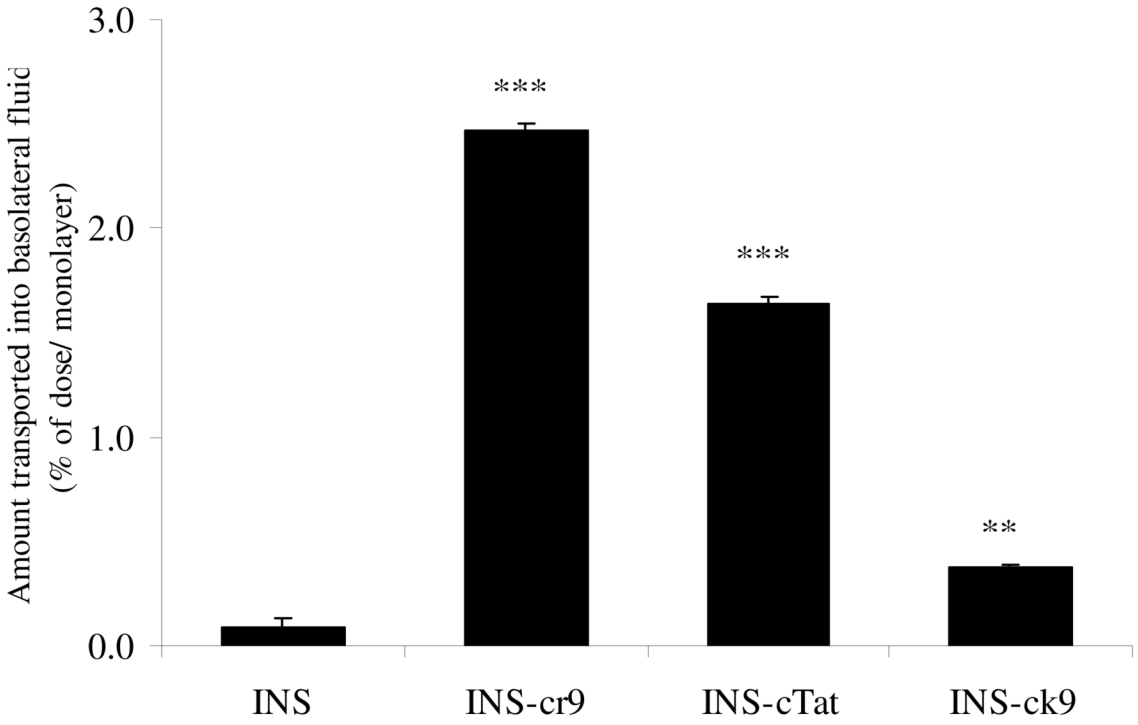

Figure 3.
Absorption of intact fraction of radiolabeled INS, INS-cr9, INS-cTat and INS-ck9, as determined by the TCA precipitation assay, across RAECM. Data are presented as mean ± SD (n = 3). ** = $p < 0.01$. *** = $p < 0.001$.

[A]

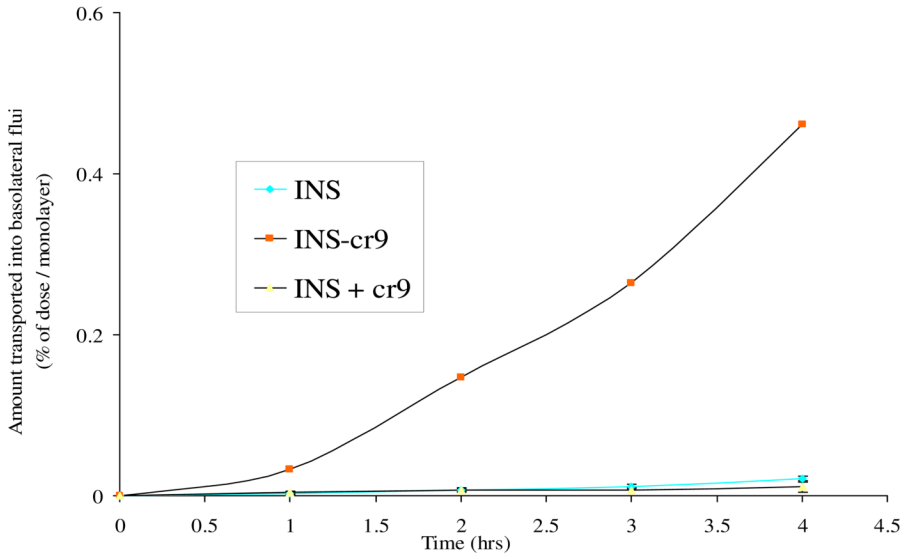

[B]

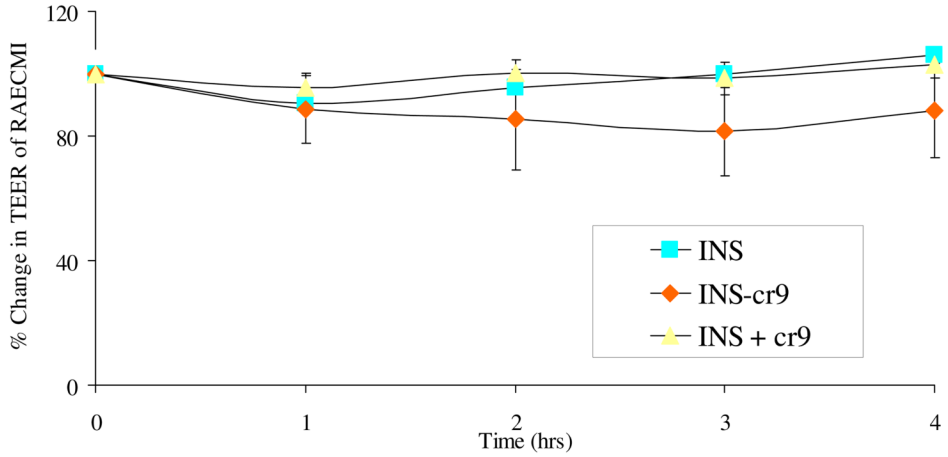

Figure 4.

[A] Time-dependent absorption of INS, INS-cr9 or a mixture of INS and cr9 at a 1:1 ratio (INS +cr9) across RAECM. Data are presented as mean±SD (n=4). **[B]** Change in transepithelial electrical resistance (TEER) of RAECM treated with INS, INS-cr9 or (INS+cr9) for up to 4 h after apical instillation. Data represent changes expressed as percentage of TEER at t = 0. Mean ±SD (n = 4) are shown.

[A]

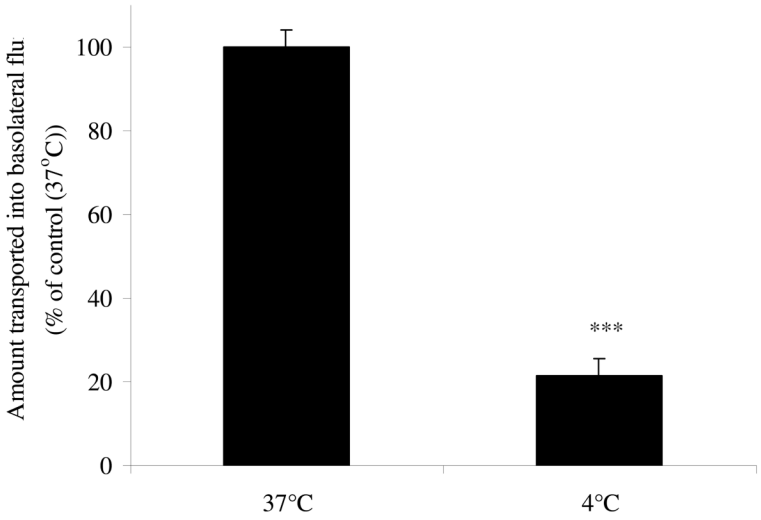

[B]

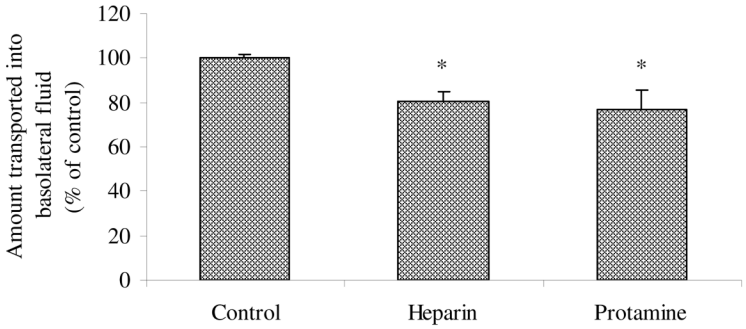

Figure 5.

[A] Effect of temperature on INS-cr9 absorption across RAECM. Absorption of intact INS-cr9 was determined following 2 h incubation of monolayers with INS-cr9 at either 37°C or 4° C. **[B]** Effect of solute charge on INS-cr9 absorption across RAECM. Monolayers were treated for 0.5 h with 1 μM heparin (negatively charged) or protamine (positively charged) prior to dosing for 2 h, during which time INS-cr9 was present as well. Data shown represent mean ±SD (n = 3–4). * = $p < 0.05$.

[A]

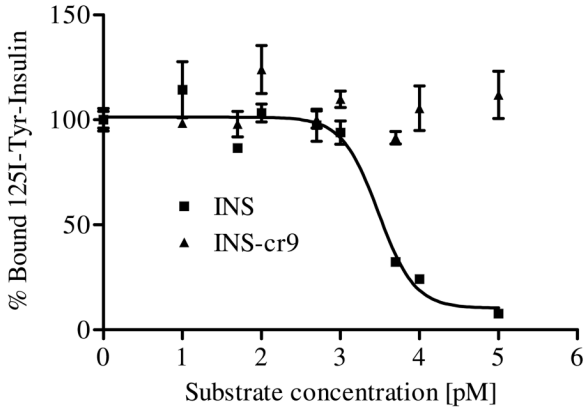

[B]

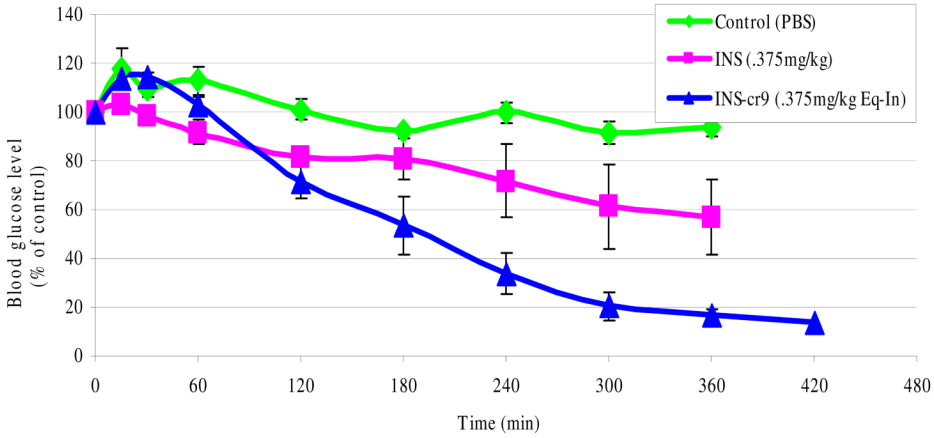

Figure 6.

[A] Inhibition of ^{125}I-INS binding to HepG2 cells by unlabeled INS and INS-cr9 conjugate. Results shown are mean±SE (n = 3). **[B]** Time courses of changes in blood glucose levels after intratracheal instillation of INS (0.375mg/kg), INS-cr9 (0.375 mg/kg with an equivalent amount of INS) or PBS in fasted and STZ-induced diabetic rats. Results shown are mean±SE (n = 3).

Table I

Sequences of cell-penetrating peptides utilized in this study. Molecular weight and pI were obtained using tools from www.expasy.org.

Cationic CPP	Sequence[a]	MW[b]	pI[c]
cTat	c-r-k-k-r-r-q-r-r-r	1442.76	12.30
cr9	c-r-r-r-r-r-r-r-r-r	1526.84	12.54
ck9	c-k-k-k-k-k-k-k-k-k	1274.72	10.55

[a] Lower case letters represent D-isoform of amino acids

[b] **MW:** Average molecular mass

[c] **pI:** Isoelectric point

Table II

Effects of various agents on INS-cr9 absorption across RAECM.

Treatment	Concentration	Transport (% of control)
Control		100 ± 6
NaN_3 + deoxyglucose	10 mM + 6 mM	85 ± 2 *
NH_4Cl	50 mM	113.8 ± 10
Monensin	30 μM	96.7 ± 5
Nocodazole	33 μM	142 ± 12 *
Chlorpromazine	30 μM	91 ± 15

Values are mean±SD (n = 4).

* statistical difference from control ($p < 0.05$).